JOURNAL OF MATERIALS SCIENCE 12 (1977) 1451–1462

Effect of impurities on the strengthening of CaF_2 single crystals

M. N. SINHA, P. S. NICHOLSON
Department of Metallurgy and Materials Science, McMaster University, Hamilton, Ontario, Canada

The critical resolved shear stress (CRSS) of pure and aliovalently doped (with Y^{+3} and Na^{+}) CaF_2 single crystals have been measured in compression along [1 1 1] axis between room temperature and 873 K. Strain rate cycling and/or stress relaxation experiments were performed to obtain the necessary parameters for the determination of rate-controlling mechanism for plastic flow. The measured temperature and concentration dependences of the activation parameters suggest that the elastic interaction of dislocations with impurity cation–lattice anion defect pairs determine the CRSS as in alkali halide crystals. The CRSS for CaF_2 single crystals doped with trivalent Y^{+3} were found an order of magnitude larger than those doped with the monovalent Na^{+}. Based on the valence of dopant cations and the magnitude of hardening produced, solution hardening in CaF_2 could be divided into two groups: "rapid" and "gradual" hardening.

1. Introduction

Experimental investigations of the low temperature plastic deformation in ionic solids in the past have largely concentrated on the sodium chloride type materials. This emphasis, which is clearly reflected in the literature, is justifiable on the basis of the simple slip geometry of this class of materials because of which they were considered ideal systems for the study of dislocation plasticity. However, an exception is the fluorite type materials with predominant ionic bonding, e.g. CaF_2. Although the slip morphology of the fluorite group halides is known for quite some time, it is only in recent years that some further studies have been done to understand its plastic behaviour [1, 2]. In CaF_2 single crystals, the apparent sensitivity of the extrageneous and added impurity influencing the dislocation mobility characteristics have been noted by several workers [3–6]. The role of impurity ions has been claimed to dominate in controling the plastic deformation, though this conclusion does not appear to be fully substantiated.

The present investigation reports a study of the effects of small and controlled additions of aliovalent impurities on the low temperature deformation mechanism of CaF_2 single crystals. For the purpose of delineating the role of impurity, the parameters of thermally activated flow have been analysed as a function of temperature, impurity concentration and strain. However, for a quantitative consideration of the solid solution hardening, most theories require the flow stress and thermal activation parameters to be evaluated at 0 K. Since the measurements at cryogenic temperatures were not feasible with CaF_2 crystals because of their brittleness, the emphasis is placed on correlating the various parameters with impurity concentration effects. The well documented literature on point defects in CaF_2 doped with YF_3 and NaF and their success in predicting various physical constants [7] suggests that these systems can be very suitable for the investigation of the mechanical behaviour in relation to defects in fluorite crystals.

2. Materials and experimental techniques

CaF_2 single crystals doped separately with different amounts of YF_3 and NaF, used in this

investigation, were grown in purified argon atmosphere by the Czochralski technique. The starting material was optical grade purity CaF_2 (from Harshaw Chemical Co.) in chunk form. All of the dopants (purity >99.99%) were individually added to the molybdenum crucible in powder form beforehand. The crystals of Harshaw were used as both seed and base materials and other details of the crystal growing procedure were the same as that described by Hiller and Stafsudd [8]. All of the crystal boules were grown on ⟨1 1 1⟩ seeds

Following growth, the boules were wrapped in molybdenum foil and sealed separately in quartz tubes after evacuating them to 10^{-5} torr and filling with ultra-pure argon. Each of them was annealed at 900° C for 48 h. Impurity segregation present in the as-grown boules was observed to disappear following this treatment. Finally each boule was annealed in a monel tube furnace in HF gas for 3 to 4 h at the above temperature to remove oxygen [9]. Crystals were slowly cooled to room temperature at 5° C min^{-1}. The concentration of dopants was estimated using atomic absorption spectroscopy, X-ray fluorescence and neutron activation techniques. The limits on the analysed values are standard deviations based on three measurements on each crystal after final anneal. The composition of the crystals studied are listed in Table I together with symbols used in all figures for convenience.

Test specimens were cut from the central portion of the crystal boules to a size of 3.5 mm × 3.5 mm × 7.5 mm using a precision wafering machine taking {1 1 1} cleavage as the reference. The specimens were ground flat on metallographic papers using a V-block, taking care to make the ends true and parallel, and then chemically polished in hot sulphuric acid to remove at least 0.5 mm surface damage due to cutting and grinding.

The samples were deformed in compression along a [1 1 1] direction† in an Instron universal testing machine at a base strain rate of 1.2×10^{-4} sec^{-1}. Two types of tests were performed: the standard stress relaxation and the strain rate cycling. At low temperatures (<100° C), where the limited ductility of the specimens restricted the use of the strain rate change technique, the stress relaxation technique was used. The data from both types of tests performed at difference temperatures were used to evaluate the activation volume and activation enthalpy for yielding and plastic flow.

TABLE I Chemical analysis and dopant concentration symbols used

YF_3 doped crystals	NaF doped crystals
◇ 26 at.ppm (2.6×10^{-3} at.%)	♦ 125 at.ppm (12.5×10^{-3} at.%)
△ 64 at.ppm (6.4×10^{-3} at.%)	▲ 865 at.ppm (86.5×10^{-3} at.%)
○ 81 at.ppm (8.1×10^{-3} at.%)	● 1260 at.ppm (12.6×10^{-2} at.%)
□ 255 at.ppm (25.5×10^{-3} at.%)	■ 2431 at.ppm (24.31×10^{-2} at.%)

Analysis of base material: Al = 5, Mg = 10, Si < 10, Y = 5, Na = 10 (wt.ppm), symbol used, +.

3. Results

3.1. The temperature dependence of yield stress

The effect of trivalent and monovalent impurities on the temperature dependence of the shear yield stress, τ_y (taken as the 0.1% offset proof stress) was determined between 300 and 873 K. These are shown in Figs. 1a and b respectively for Y^{+3} and Na^+ doped crystals. While for the undoped (pure) crystals there was only a modest increase in τ_y with decrease in temperature, τ_y for the doped crystals increased sharply with decreasing temperature and increasing impurity content. Separating the CRSS into a thermal (or effective) stress component τ^*, and an athermal (or internal) stress component τ_μ,

$$\tau_y = \tau^* + \tau_\mu, \quad (1)$$

it can be seen that the doping treatment has resulting in a large increase in τ^* compared to the increase in τ_μ. In each system however, the experimental τ_y–T curves approach asymptotically to a temperature independent region anticipated for athermal behaviour. The critical temperature T_c, below which the yield stress is temperature dependent, is observed (Fig. 1) to be in the neighbourhood of 750 K. Since Figs. 1a and b do not allow one to be so precise, employing a more logical method of arriving at T_c values by using the plots of the slops, $\partial\tau_y/\partial T$ of the curves of Fig. 1 against

†The [1 1 1] crystallographic axis was chosen because it is known to be the softest orientation for the fluorite lattice [10, 11], and also for ease in preparation due to easy cleavage. In this orientation, the {1 0 0} [1 1 0] type primary slip planes correspond to a Schmid factor of 0.47 [10].

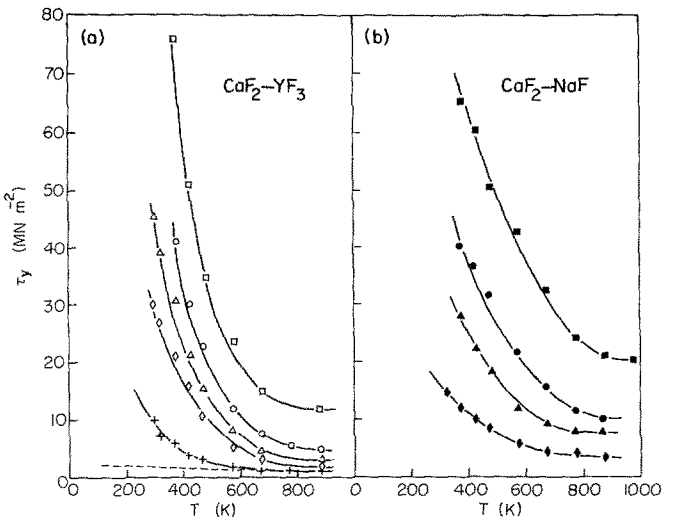

Figure 1 Temperature dependence of CRSS of pure and doped CaF_2 single crystals (a) doped with Y^{+3}, (b) crystals doped with Na^+.

temperature T (which approximated to straight lines for $T > 423$ K) a T_c value of 750 (±10 K) could be placed for all crystals except the two high-doped ones of CaF_2–NaF system (Fig. 2)†. For these two compositions, the transition temperatures are 860 and 950 K respectively, increasing slightly with increase of concentration. The reasons for this increase of T_c is not precisely clear. It could be due to changes in the elastic modulus as observed in metallic systems [12]. Neglecting the small variation of shear modulus μ‡ with temperature (shown by dotted line in Fig. 1a) τ_μ is taken from the flat portion of τ_y–T diagram in Fig. 1 where $\partial\tau_\mu/\partial T = 0$ corresponding to the above T_c values. To substantiate the validity of the assumption of Equation 1, i.e. τ_μ measured by a given experimental technique, versus the physical quantity τ_μ of Equation 1; τ_μ values utilizing one specimen of the same composition were determined from saturation of relaxed stress, using stress relaxation tests. The stress at which the relaxation rate was almost zero was taken as a measure of τ_μ [14, 15]. There was good agreement in both sets of internal stress values within the experimental error limits.

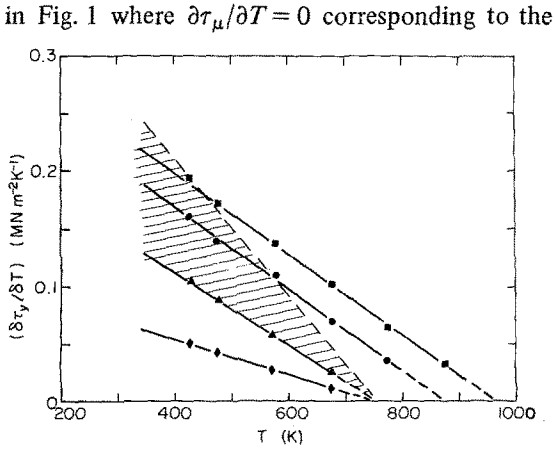

Figure 2 Variation of the temperature dependence of the CRSS for Na^+ doped crystals. Superimposed upon the continuous lines, the hatched area represents the region of similar data points (family of converging straight lines) obtained for Y^{+3} doped crystals.

3.2. The activation volume

The activation volume V^* was obtained using the relationship

$$V^* = kT\left(\frac{\partial \ln \dot{\epsilon}}{\partial \tau^*}\right)_T \qquad (2)$$

where k = Boltzmann's constant, T = absolute temperature in K, $\partial \ln \dot{\epsilon} = \ln \dot{\epsilon}_2/\dot{\epsilon}_1$, $(\dot{\epsilon}_2/\dot{\epsilon}_1 = 10)$, and $\partial\tau^*$ = change in stress during change of strain rate from $\dot{\epsilon}_1$ to $\dot{\epsilon}_2$. From stress relaxation tests at low temperatures, V^* was calculated using [16, 17]

$$V^* = MkT[\partial \ln(-R\dot{\sigma})/\partial\sigma]_T, \qquad (3)$$

where M is the Taylor factor, R is the rigidity of the deformation machine (obtained from the slope of elastic portion of the stress-strain curve), $\partial(-\dot{\sigma})$ and $\partial\sigma$ are the slopes and stresses at two times along the stress relaxation curve respectively. To determine whether the activation volume determined by this means, as well as that of

†The data points shown in Fig. 2 are for the Na^+ doped crystals; the hatched area represents the regions where the data for all Y^{+3} doped crystals fall (similar set of converging straight lines), and have been left out for clarity.

‡In the absence of shear modulus data for CaF_2 beyond 300 K [13], μ is assumed to vary in the same linear fashion up to 900 K.

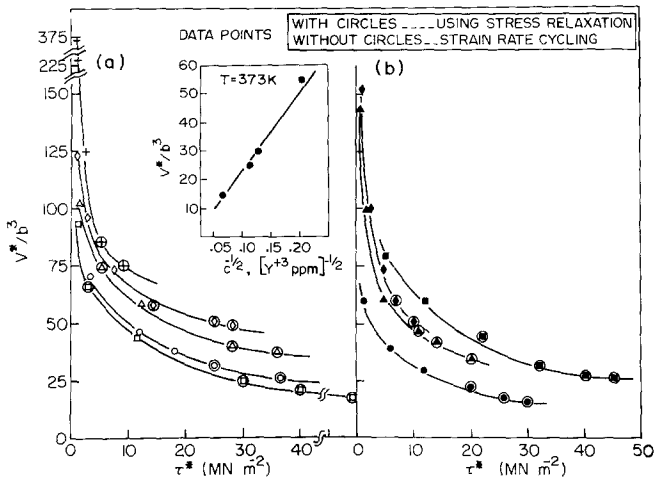

Figure 3 Activation volume as a function of effective stress and concentration.

Equation 2, remained independent of deformation stage, stress relaxation and strain rate change were performed at increasing amounts of plastic strain. There was good reproducibility in the stress relaxation behaviour and $\Delta\tau$ remained constant and independent of plastic strain, suggesting that V^* is not a function of plastic strain in the systems examined.

The results of the measurements of V^* are given in Fig. 3 where V^*/b^3 (b is the Burgers vector = 3.86×10^{-8} cm) is plotted against τ^*, the effective stress. It is seen that the data obtained by the two techniques are consistent over the entire stress range for both the Y^{+3} and Na^+ doped crystal systems. The magnitude of V^* generally decreases continuously with increasing concentration of impurities in both systems, except for the Na^+ doped crystal containing highest concentration of 24.31×10^{-2} mol% (Fig. 3b). For Y^{+3} doped crystals, $V^* \propto c^{-1/2}$ (inset of Fig. 3a), but no such simple relationship could be found for the data on Na^+ doped crystals (c being the impurity concentration in at. ppm).

3.3. The activation energy ΔH

The values of activation energy ΔH were obtained from the slope of the plots of Fig. 1 using the relation

$$\Delta H = -V^* T(\partial\tau^*/\partial T)_{\dot{\epsilon}}, \qquad (4)$$

where V^* is the experimental activation volume.

Fig. 4 shows the dependence of ΔH on temperature T. In the case of Y^{+3} doped crystals all the data points approximate a single straight line (Fig. 4a) and is a reflection of the operation of a single thermally activated mechanism. The total activation enthalpy, ΔH_0 (ΔH at $T = T_c$) required to surmount the barrier is read from Fig. 4a as 0.95 eV. Fig. 5a shows the variation of ΔH against τ^*. A constant value of ΔH_0 (ΔH at $\tau^* = 0$) of 0.93 eV obtained for Y^{+3} doped materials which is similar to $\Delta H_0 = 0.95$ eV found from Fig. 4a. Figs. 4b and 5b give the same data for the Na^+ doped crystals. The activation energy increases linearly with temperature

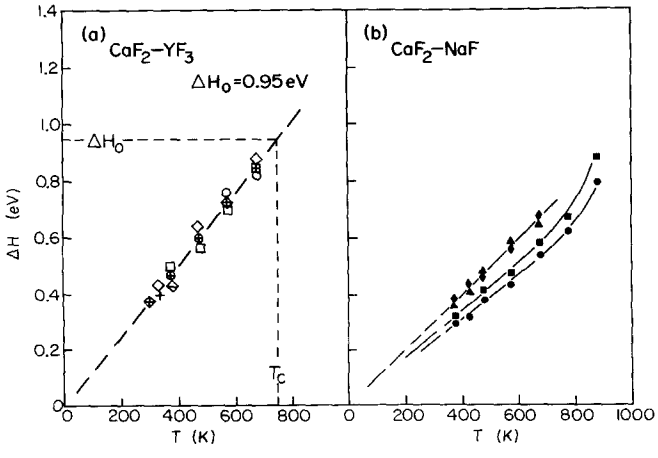

Figure 4 Activation energy as a function of temperature.

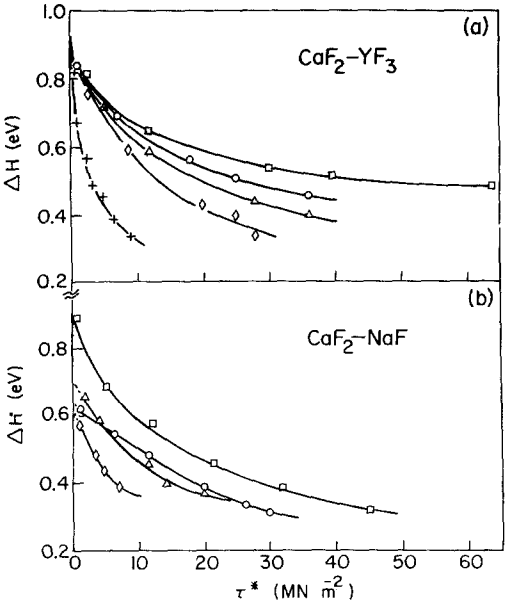

Figure 5 Activation energy as a function of effective stress and dopant concentration.

(Fig. 4b). However, since T_c depends on impurity concentration, the value of the total energy ΔH_0 (ΔH at which $\tau^* = 0$) increases from 0.65 eV in crystals containing low Na^+ to 0.90 eV in crystals with maximum of 24.31×10^{-2} mol % Na^+ (Fig. 5b).

4. Discussion

4.1. Doping CaF_2 with aliovalent ions

Amongst the many fluorite structure compounds which form a rare example of the ionic species containing interstitials and vacancies in very high concentrations, the systems CaF_2–YF_3 and CaF_2–NaF are perhaps the best studied examples [7]. In YF_3 doped CaF_2 crystals after annealing in HF atmosphere, excess fluorine ions provide the charge compensation by occupying nearby interstitial sites forming $(F^{+3}-F_i^-)$ dipoles. The expansion of the CaF_2 lattice depends sensitively on the F_i^- (fluorine interstitials) in proportion of one to each YF_3 mole dissolves (the solubility limit is ~50 mol %), and that there is no phase separation or disporportionation observed even on slow rates of cooling [18, 19]. Analogously, monovalent Na^+ are incorporated substitionally leading to the formation of a fluorine vacancy, F_v^-, on the nearest fluorine sublattice but the solid solubility limit and the changes in lattice parameter due to vacancies (F_v^-) in this system is much more limited. Ure [20] found a solubility limit of 0.6 mol % below 600° C. According to Tressler [21], NaF is soluble in CaF_2 up to a maximum of ~2 mol % at 820° C. The amount of impurities in the present work (i.e. 25.5×10^{-3} mol % maximum of YF_3 and 24.31×10^{-2} mol % maximum of NaF) are below these levels and therefore should be in solid solution. However, the slow cooling employed may give rise to an impurity agglomeration effect in the Na^+ doped crystals. The effect was still not large enough to play a role in producing serrated type of flow behaviour up to the temperature range considered.

4.2. Application of rate theory approach

The use of rate theory to analyse thermally activated movement of dislocations have been extensively discussed and reviewed (see [22] for an elegant treatment). The thermally activated deformation rate $\dot{\epsilon}$ at low temperature is usually described by an equation of the form

$$\dot{\epsilon} = \dot{\epsilon}_0 \exp(-\Delta G/kT) \qquad (5)$$

where $\dot{\epsilon}_0$ is a pre-exponential factor which includes the number N of activatable sites per unit volume, the area A swept out by a dislocation segment subsequent to successful activation and ν is the frequency of vibration of the dislocation segment.

To avoid having to show how the factor $\dot{\epsilon}_0$ could be internally dependent and/or varying with stress and temperature, it has been assumed constant. The anomalous behaviour, if any, of other experimentally measurable parameters, namely V^*, τ^* and ΔH have instead been checked for their consistency as described. If one single mechanism should be exclusively rate-controlling, the dislocations having overcome one barrier by thermal activation must face the same type of obstacles again. It follows then that the total activation enthalpy, ΔH_0 must remain constant and independent of temperature and effective stress. Likewise, there should be no discontinuity or break observed in the V^*–τ^* and ΔH–T plots. From the contents of Figs. 3 and 4 the conditions of a smooth variation of V^* and ΔH against τ^* and T respectively are held quite satisfactorily for all the compositions studied. A constant value of ΔH_0 is obtained in the case of CaF_2–YF_3 system independent of concentration. Thus it can be concluded that a single thermally activated mechanism controls the deformation in the Y^{+3} doped CaF_2 single crystals.

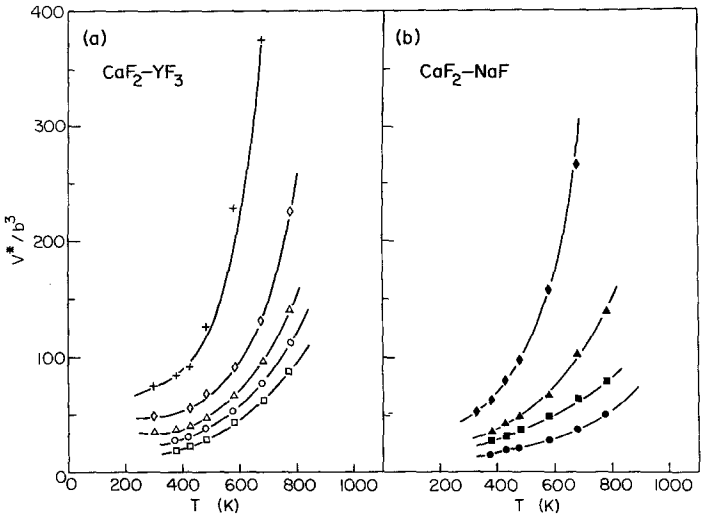

Figure 6 The temperature dependence of activation volume.

The result on the CaF_2–NaF system however, shows a different behaviour. Figs. 3b, 4b and 5b show the activation volume and activation energy as a function of effective stress and temperature. It can be seen from these results that in crystals containing the maximum concentration of Na^+, activation volume has increased instead of the general decreasing behaviour observed in all other compositions. It can be argued that the hardening effects of the Na^+ ions dissolved in the CaF_2 lattice reach a limiting value, and the potency of individual solute atoms in the form of Na^+–F_v^- dipoles as barrier to dislocation motion are no longer valid. This does not necessarily indicate that the actual rate-controlling mechanism has changed, and this can also be seen if the activation volume is plotted against temperature as in Fig. 6; there are no discontinuities in the behaviour.

4.3 Solid solution hardening

One basic result on the strengthening behaviour of CaF_2 of the present work namely the strong dependence of τ^* and V^* on concentration of solute ions should be noted. It is well known that while the intrinsic lattice friction controlled mechanisms (such as Peierls type) would not result in any appreciable concentration dependence of τ^* and V^*, the dispersed barrier type of mechanism would. A unique feature of the Peierls type mechanism is the small activation volume, V^*/b^3 of the order of 20 [23]. The impurity mechanism is also characterized by small activation volume, but the theory of Peierls mechanism predicts it to be independent of the state and dispersion of impurities. The experimental results obtained in the present work therefore disqualify the lattice friction as the probable rate controlling mechanism. Further, since the activation volume remains independent of plastic strain, other structure-sensitive mechanisms such as cross-slip, jog dragging and forest intersection, must also be eliminated.

Alternative approaches to the strengthening mechanism are all based on the concept of dislocation interactions with solute atoms [24–27]. Central to all of these models is the idea that aliovalent ions as point defects in ionic solids are accompanied by appropriate lattice defects to maintain overall charge neutrality of the crystal. The point defects are described as elastic dipoles which interact with both edge and screw dislocations in a thermally activated process. These have to be overcome for plastic flow to occur. The dipoles can cluster to form multiple dipoles and, depending upon phase equilibria and heat treatment conditions, develop to an increasing size of the discs of precipitates of the second phase.

If the fluorine ions (interstitials or vacancies) are associated with dopant cations and accompany an anisotropic strain field, Fleischer's model [24] implies that they can be important for hardening in ionic crystals since this model is based on the strong elastic interaction between such defects and dislocations. Fleischer calculated the elastic interaction energy of the defect in the stress field of a screw dislocation and maximized the derivative of the energy with respect to distance along the slip plane to obtain the maximum force on

the dislocation. In an analogous manner, Chang and Graham [28] calculated the interaction energy between an edge dislocation and a non-symmetrical defect. Nadeau [29] using a graphical method showed that the nature of the resulting force-distance curves for the short range interaction between edge dislocation and the tetragonal defect are very similar (at least qualitatively) to the one for screw dislocation. The maximum force of interaction in both cases arises at a distance of one Burgers vector and sharply decays at about 2 to 3b. The force distance curve for an edge dislocation in the fluorite type crystals with {100}[110] slip system does not seem to have been explicitly published. Therefore, without assuming the exact description of the maximum interaction force will remain unchanged, the possibility of strong interaction between edge dislocation and tetragonal defects cannot be ruled out.

4.3.1. The temperature dependence of effective stress

Since the deformation parameters are found to depend on the impurity concentration, it is appropriate to examine the results in the light of tetragonal hardening mechanism. According to Fleischer's treatment of this problem, the effective stress is dependent on temperature according to

$$(\tau^*/\tau_0^*)^{1/2} = 1-(T/T_c)^{1/2}; (T<T_c) \quad (6)$$

where τ_0^* is the effective stress at 0 K such that

$$\tau_0^* = A\mu b\,\Delta\epsilon\, c^{1/2} \text{ and } T_c = (F_0 b/\alpha K) \quad (6a)$$

in which A is the proportionality constant depending on the relative orientation of the defect and the dislocation, μ is the shear modulus, $\Delta\epsilon$ is the tetragonality of the defect's strain field, c is the impurity concentration, F_0 is the interaction force at 0 K and α is a constant.

Fig. 7 shows that Equation 6 is obeyed quite satisfactorily for the Y^{+3} doped crystals. The slope of straight lines also agrees with the theoretical prediction that it should vary as $c^{1/4}$ [24] (inset of Fig. 7). The data of the Na^+ doped crystals could not be represented with similar accuracy by such a relation. The precise value of τ_0^* (τ^* at 0 K) is uncertain because it involves extrapolation of τ^* to 0 K from Fig. 1. Experimentally, the data on τ^* in the present materials are difficult to obtain anywhere near 0 K. However, by extrapolation of the straight line plots of Fig. 7, values of τ_0^* of 56.3 MN m^{-2} for undoped (so-called "pure") crystals and 190, 270, 360.5 and 560 MN m^{-2} are obtained for the four Y^{+3} doped crystals. From this, τ_0^* is found proportional to

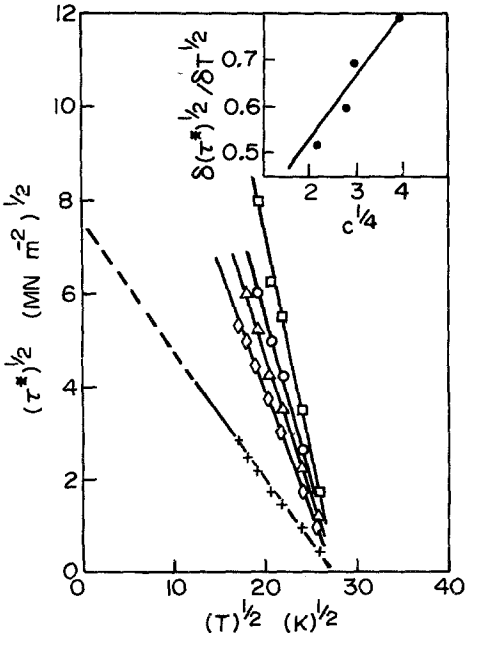

Figure 7 Plots of $(\tau^*)^{1/2}$ against $(T)^{1/2}$ for pure and Y^{+3} doped CaF_2 single crystals. Inset: the variation of slopes of straight lines against (concentration)$^{1/4}$.

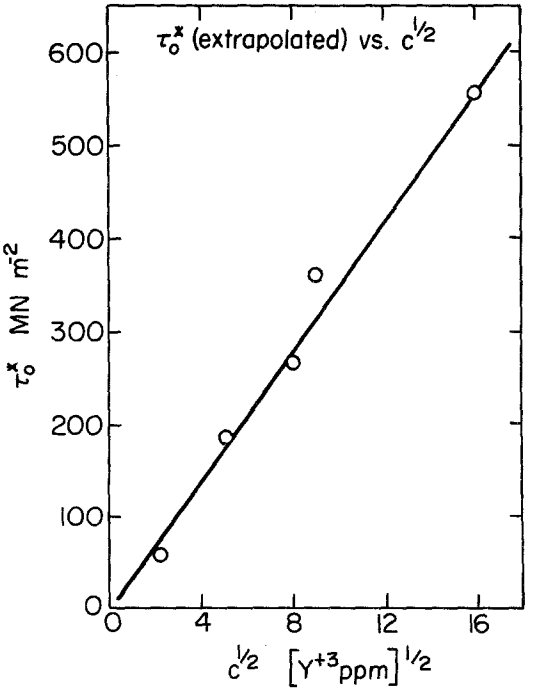

Figure 8 τ_0^* (extrapolated values from Fig. 6) versus concentration)$^{1/2}$ for Y^{+3} doped crystals.

$c^{1/2}$ (Fig. 8), when taken together the Y^{+3} content for undoped crystal. The results thus suggest that the temperature dependence of flow stress and solid solution hardening effects in trivalently yittrium doped CaF_2 single crystals can be explained in terms of the tetragonal hardening mechanism. Further, since $\tau_0^* \propto c^{1/2}$, it is not unreasonable to assume that dislocations interact with single obstacles in this case.

The flow stress at 0 K is determined by the force F_0 required to break through the obstacle:

$$F_0 = \tau_0^* b l \tag{7}$$

where τ_0^* is the effective stress at 0 K and l is the obstacle spacing. A reasonable assumption for the effect of stress and temperature on l is the Friedel relation [30]:

$$l = \left(\frac{2E_l}{Nb\tau^*}\right)^{1/3} = \left(\frac{\mu b}{N\tau^*}\right)^{1/3} \tag{8}$$

in which E_l is the line tension of the dislocation ($\mu b^2/2$ assumed isotropic) and N is the area density of obstacles which depends on the assumptions made about the average number and distribution of solute atoms on the participating slip planes. In ionic solids any aliovalent impurities which are not isovalent will be paired with one vacancy (or interstitial) of opposite charge to maintain charge neutrality. For fcc lattice of CaF_2 with $\{100\}[110]$ slip system, if a is the lattice constant, the area density on one slip plane is $2c/a^2$. In terms of slip dimension this equals $4c/b^2$. Following Fleischer [24], if only two-thirds of the defects are allowed to interact with a dislocation, in the two atomic planes bordering the dislocation, then $N = (2/3) \times 2 \times (4c/b^2) = 5.3\ c/b^2$. This, when substituted in Equation 8 with Equation 7 gives

$$F_0 = 0.574 b^2 (\tau_0^*/c^{1/2})^{2/3} (\mu)^{1/3} \tag{9}$$

The value of the constant F_0 can thus be obtained from the slope of plot of Fig. 8. This slope is measured to be $\tau_0^*/c^{1/2} = 52 \times 10^3$ MN m^{-2} which, with $\mu_0 = 5.95 \times 10^4$ MN m^{-2} [13], gives $F_0 = 42.5 \times 10^{-10}$ N. In terms of the breaking angle (ϕ) concept of hardening due to Foreman and Meakin [31]

$$F_0 = 2E_l \cos(\phi_0/2) \tag{10}$$

where ϕ_0 is the breaking angle at the obstacles at 0K. Substituting for E_l and using $F_0 = 42.5 \times 10^{-10}$ N gives $\phi_0 = 129.5°$, which is of the order of magnitude expected for solute pinning points when the obstacles are relatively weak, i.e. dislocations remain fairly straight and break-away occurs before Orowan condition is reached. Since F_0 essentially represents the distortion parameter given by $F_0 = \mu b^2 \Delta\epsilon/\text{constant}$, it is interesting to note that the F_0 value calculated here is about four times the magnitude of values obtained with NaCl type crystals [32]. This is in accord with recent results of Arsenault and DeWitt [33] who found that the total interaction force with a non-symmetrical defect is greater for an edge dislocation than with a screw dislocation. This supports previous etch-pitting results [2, 4] that the edge dislocations move slower in CaF_2 and hence should be responsible in controlling the flow stress.

While the reasonable agreement between theory and experiment only demonstrates the similarity of the force–distance curves assumed in the analysis, it does indicate, in the light of other experimental results on CaF_2 [2, 5, 6], that impurities play a definite role. The exact nature of the interaction between edge dislocations and non-symmetrical defect, however, is not yet known.

The data on the Na^+ doped crystals are not consistent enough to undertake an equivalent analysis. In this system, T_c values are found to differ as the concentration increases and no definite procedure could be used to obtain τ_0^*. Applying Frank's refined version [27] of tetragonal distortion model, it can be demonstrated that the agreement exists with experimental results for the Na^+ doped crystals, in which case it seems possible (since much limited solid solubility and slow cooling were employed) that with increasing concentration clustering or agglomeration of the dipoles might be expected. The CRSS in this case is determined by the forces which are necessary for slip dislocation to by-pass the complex during thermal activation. It should be recognised that the description of solid solution hardening of ionic cubic crystals on the basis of strong localized interaction (such as those normally characterized by the case when the barriers as a single solute atom are overcome individually); both the Fleischer and Frank theories dictate the same type of linear $\sqrt{\tau^*} - \sqrt{T}$ and $\tau^* - \sqrt{C}$ dependences. In such cases it is practically impossible to distinguish between the two [34]. The theoretical expressions of Frank's

model [27] used here apply with the assumption that dipoles even if in the agglomerate form would give rise to strong localised interaction with the dislocations.

The temperature dependence of effective stress according to this theory is given by

$$T = A - B\chi(\tau^*) \quad (11)$$

where

$$\chi(\tau^*) = \tau^*(C/\sqrt[3]{\tau^* - 1}) \quad (12)$$

The constants A, B and C are defined as

$$A = \Delta G_0/k \ln (\rho_m b^2 \nu_D/\dot{\epsilon}) \quad (13a)$$

$$B = b^3 d/\sqrt{c_{eff}} k \ln (\rho_m b^2 \nu_D/\dot{\epsilon}) \quad (13b)$$

$$C = (\sqrt[3]{2} + 1/\sqrt[3]{4}) \sqrt[3]{A/B}, \quad (13c)$$

where ρ_m = mobile dislocation density, ν_D = Debye frequency, c_{eff} = the effective concentration of obstacles, d = distance of the centre of the dipole from the slip plane and other terms are as previously defined.

Fig. 9 presents the data of Fig. 1b evaluated by means of Frank's equation in a T–χ diagram. The choice of constant C between 5 to 9 $(MN\,m^{-2})^{1/3}$ gives the best agreement with the results, subject to the constraint that the points calculated from Equations 11 and 12 still fall on a straight line. From the given relationships for constants A and B in Equation 13,

$$A/B = \Delta G_0 \sqrt{c_{eff}}/b^3 d \quad (14)$$

The experimental values of the constants A and B are given by the intercepts in (K) and slopes in $K\,m^2\,MN^{-1}$) of the plots in Fig. 9, respectively. The intersection with the temperature axis is a measure of the Gibbs free energy, ΔG_0 according to Equation 13a. At the same time the intercept is the temperature T_c where the obstacles are overcome entirely by thermal activation. The concentration c_{eff} can be evaluated using Equation 14 (d is assumed to be 1) from the known experimental values of A and B out of Fig. 9. The values of the constants in Equation 13 and the calculated c_{eff} (using Equation 14 and experimental ΔG_0 from Fig. 5b) are listed in Table II. It is observed that the agreement between the experimental T_c and c values and those derived from the theory is much better than would be expected in view of the approximations that were necessary in deriving these plots.

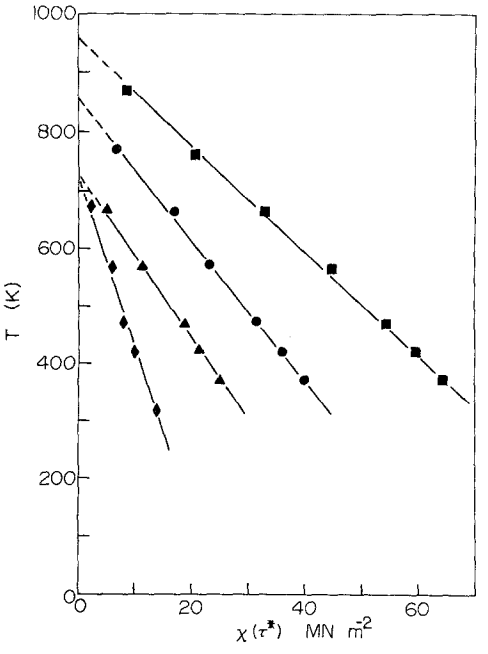

Figure 9 Plot of $\chi(\tau^*)$ against temperature for Na^+ doped crystals.

Several other types of interactions have been suggested between solutes and dislocations that deserve mention. The major ones are (i) effect due to differences in elastic constants (ii) size effect (including effects due to both dilatational and shear distortions) and (iii) electrostatic interaction. Since there is no data available on the effect of any kind of impurities on the elastic constants of

TABLE II Na^+ doped CaF_2 crystals

Na^+ (mol. ppm.)	Values of the constants A, B and C derived from experimental data			c_{eff}.ppm (calc)	T_c(K)	
	A(K)	B(K m² MN⁻¹)	C(MN m⁻²)$^{1/3}$		from Fig. 2	from Fig. 9
125	725	30.2	5.0	207	750	725
865	727	15.24	6.2	823	760	727
1260	860	12.0	7.0	1697	865	860
2431	960	7.7	8.5	2372	960	960

CaF_2, no exact assessment of this effect can be made. The size effect can also be excluded since the ionic radii of Y^{+3} and Na^+ in the present examples differ very little (0.93 and 0.95 Å respectively). The electrostatic interaction may have a possible role, but at present there is some difficulty in explaining the whole of the low temperature strength only due to electrostatic forces [26, 35].

4.3.2. The concentration dependence of effective stress

In most of the single barrier models of hardening the obstacles to dislocation motion are mainly individual atoms. Labusch [36] has proposed a statistical theory of solid solution hardening and considered the obstacles to be groups of solute atoms. Both of these theories suggest a power law $\tau^* \propto c^n$; exponent $n = \frac{1}{2}$ for obstacles of Fleischer type with a local stress field of tetragonal symmetry and $n = \frac{2}{3}$ for obstacles with an extended stress field after Labusch. In Fig. 10 the experimental data of τ^* at 373 K were compared with the theoretical curves drawn using Fleischer's and Labusch's solid solution strengthening theories. Although there are not sufficient data points, the stress increase upon doping with Y^{+3} exactly obeys the $\frac{1}{2}$ power law in Fleischer's theory. The intercept of the straight line gives $\tau^* = 6.4\,MN\,m^{-2}$ which agrees very well with τ^* (undoped) of $6.0\,MN\,m^{-2}$ measured experimentally. From this and the results of previous section, it can be concluded that the strengthening of CaF_2 upon doping with Y^{+3} (producing fluorine interstitials, F_i^- defects) in the composition range considered occurs by the interaction of dislocations with individual Y^{+3}–F_i^- dipoles i.e. according to Fleischer–Friedel model. In this case, the deformation kinetics are described reasonably well by the Arrhenius-type equation with an activation enthalpy relatively independent of temperature and impurity concentration.

The data on the Na^+ doped crystals fit Labusch's theory rather better (Fig. 10), but there is some difficulty in the absolute value. Frank and Rappich [35] assert that with extremly small concentration range the dipoles would not cluster even under slow cooling, and therefore the thermal pretreatment will have practically no effect. Accordingly, a $c^{1/2}$ dependence in small range of concentration is expected. This seems to be valid from the dashed line shown in Fig. 10, excluding the point for highest Na^+ concentration. Thus there is a change in concentration dependence of τ^* from c^n (n between $\frac{1}{2}$ to $\frac{2}{3}$) to c. At present no explanation can be given for this behaviour. One may expect that when the concentration of short range barriers increases to a critical value the dislocation flexibility becomes limited, so that the hardening rate increases as a consequence of finite dislocation flexibility. Direct calculation of the flow stress in computer simulation studies by Ono [37] indicates that the exponent n in $\tau^* \propto c^n$ could vary over a range of values with 0.3 to 0.7 depending upon the strength and nature of localised interaction, although these results should be considered tentative due to the assumption made to simplify the computation.

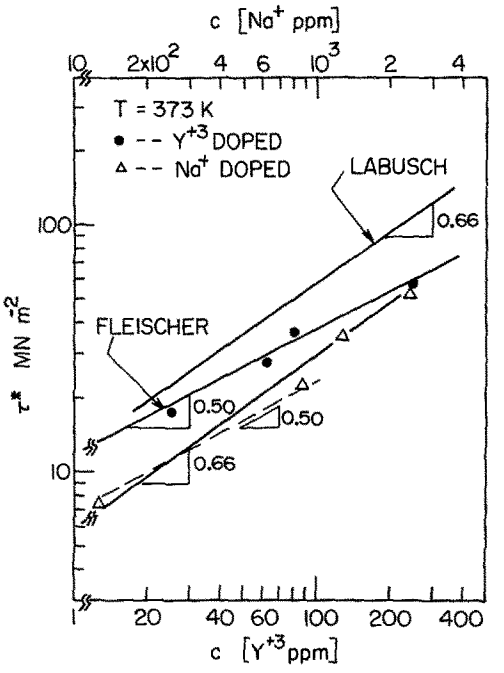

Figure 10 Comparison of experimental data against theoretical lines.

4.4. Hardening rates

Fig. 11 is used to calculate the hardening rates as a function of the concentration in both systems i.e. $\Delta\tau^*/\Delta c$ per atom of impurity. The results are given in Table III for different valent cations directly and in terms of the shear modulus μ. The hardening rate values for the various rock salt type ionic crystals are taken from literature for comparison. Monovalent cations substituting for Ca^{+2} show a low hardening rate with value of $\Delta\tau^*/\Delta c$ in the range 0.4μ. It can be noted that this value is typical of the so-called 'gradual' hardening, using the nomenclature of Fleischer [38]. In the case of CaF_2 doped with trivalent Y^{+3} the rate of harden-

TABLE III Concentration dependence of the flow stress in ionic crystals

Crystals	Defect	Typical Hardening (in terms of shear modulus, μ)
Rock salt type [38]		
KCl	F center	$\mu/2.5$
NaCl	Monovalent ions	$\mu/100$
NaCl	Divalent ions	2μ
LiF (irradiated)	Interstitial fluorine	5μ
KCl	Interstitial chlorine	7μ
MgO [35, 39]	Trivalent ions (Fe^{+3})	5.5μ
Fluorite Type (present work)		
CaF_2	Fluorine interstitial	5.7μ
CaF_2	Fluorine vacancy	0.4μ

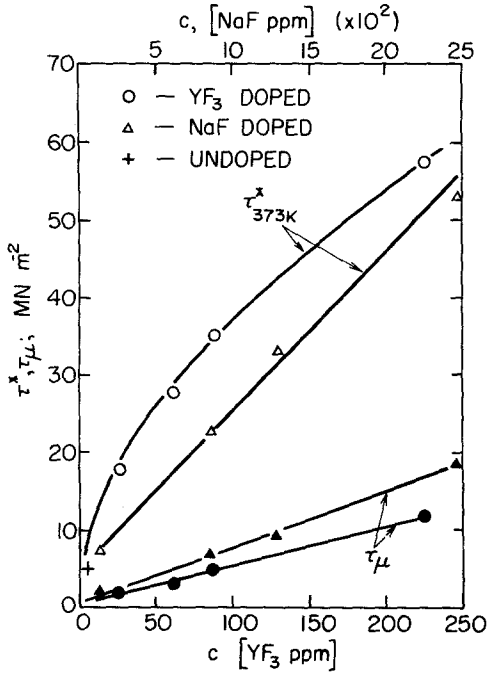

Figure 11 Solution hardening of the thermal and athermal components of flow stress by mono- and trivalent impurity ions in high purity CaF_2 single crystals.

ing is $5.7\,\mu$. This is analogous to the case 'rapid' hardening which is produced by tetragonal defects.

4.5. Athermal hardening

At higher temperatures the assumption that the dipole is a rigid defect is not necessarily valid. From Fig. 1, the CRSS appears to reach a constant minimum at approximately 800 K. However, depending upon the level of impurity concentration the athermal component (τ_μ) of the flow stress attains different values. One explanation for this has been developed by Pratt *et al.* [25] for the situation where the elastic energy of the system is lowered by dipoles reorienting in the stress field of moving dislocations. The dislocations experience a long range retarding force via the induced Snoek effect [40]. For this contribution, the theory yields

$$\tau_\mu \propto \mu \Delta\epsilon c \qquad (15)$$

The dependence of τ_μ on the impurity concentration c measured at T_c is shown in the bottom part of Fig. 11. Starting from the values of undoped CaF_2, a linear increase is found, which is consistent with the prediction of the theory in terms of increasing concentration of dipoles producing a greater drag on dislocations. If the contribution of basic purity in the undoped samples ($\simeq 1\,MN\,m^{-2}$) is separated, the straight lines in Fig. 11 pass through the origin indicating that the high temperature strengthening due to dislocation–dislocation interactions (usually represented through $\alpha\mu b\sqrt{\rho}$; α being a constant and ρ the dislocation density) is negligible. Substitution of the slope of straight lines in Fig. 11 with a proportionality constant of ~ 1.5 [25] in Equation 15 gives $\Delta\epsilon(F_i^- - Y^{+3}) = 0.63$ compared with $\Delta\epsilon(F_v^- - Na^+) = 0.18$. These values are of the order of magnitude expected and supports the general implication of dipole hardening theories that larger hardening is associated with larger strain difference $\Delta\epsilon$. The considerations of other possible mechanisms of $\Delta\tau_\mu$ such as athermal cutting of aggregates by dislocations and dislocation by-passing by Orowan looping mechanism cannot be attempted at the present time because of the absence of a precise knowledge concerning the stage of aggregation and of the lack of evidence of precipitation effects in these systems.

5. Summary

The solid solution hardening of CaF_2 single crystals by aliovalent impurity cations (Y^{+3} and Na^+) has been studied over a temperature range between

room temperature and 873 K. The temperature and concentration dependences of the critical resolved shear stress, activation volume and activation energy were examined in terms of the thermally activated deformation theory approach. The analysis of the hardening carried out has shown that the flow stress at low temperatures is controlled by impurity cation – lattice anion defect complexes, while at elevated temperatures in the 'plateau' region CRSS is determined by the induced Snoek effect of oriented dipoles in the stress filed of mobile dislocations. The rate of hardening per atom basis was found to be strongly dependent on the mode of incorporation of foreign ions and the lattice defects they produce: trivalent Y^{+3} with fluorine interstitials, F_i^- as the defect strengthens the crystals more strongly than the monovalent, Na^+ in which case fluorine vacancies, F_V^-, form.

References

1. A. G. EVANS and P. L. PRATT, *Phil. Mag.* **20** (1969) 1213.
2. *Idem, ibid* **21** (1970) 951.
3. S. R. SASHITAL and K. VEDAM, *J. Appl. Phys.* **43** (1972) 4396.
4. G. A. KEIG and R. L. COBLE, *ibid* **39** (1968) 6090.
5. R. N. KATZ AND R. L. COBLE, *ibid* **45** (1974) 2382.
6. A. A. URUSOVSKAYA and V. G. GOVORKOOV, *Sov. Phys – Cryst* **10** (1966) 437.
7. "Crystals with the Fluorite Structure", Edited by W. HAYES (Clarendon Press, Oxford, 1974).
8. M. A. HILLER and O. M. STAFSUDD, *J. Appl. Phys.* **35** (1964) 693.
9. H. GUGGENHEIM, *ibid* **34** (1963) 2482.
10. P. T. SAWBRIDGE and E. C. SYKES, *Phil. Mag.* **24** (1971) 33.
11. G. Y. CHIN and W. L. MAMMEL, *Met. Trans.* **4** (1973) 335.
12. V. A. MOSKALENKO and V. N. PUPTSOVA, *Mat. Sci. Eng.* **16** (1974) 269.
13. D. R. HUFFMAN and M. H. NORWOOD, *Phys. Rev.* **117** (1960) 709.
14. G. B. GIBBS, *Phil. Mag.* **13** (1966) 517.
15. S. R. MACEWEN, O. A. CUPCIS and B. RAMASWAMI, *Scripta Met.* **3** (1969) 441.
16. G. B. GIBBS, *Phil. Mag.* **13** (1966) 317.
17. S. P. AGRAWAL, G. A. SARGENT and H. CONRAD, *Met. Trans.* **4** (1973) 2613.
18. J. SHORT and R. ROY, *J. Phys. Chem.* **67** (1963) 1860.
19. E. G. IPPOLITOV, L. S. GARASHINA and A. G. MAKLACHKOV *Inorg. Materials* **3** (1967) 59.
20. R. W. URE Jun., *J. Chem. Phys.* **26** (1957) 1363.
21. R. E. TRESSLER, S. M. THESIS (1964), M.I.T., (U.S.A.)
22. U. F. KOCKS, A. S. ARGON and M. F. ASHBY, *Prog. Mat. Science* **19** (1974).
23. P. GUYOT and J. E. DORN, *Can. J. Phys.* **45** (1967) 983.
24. R. L. FLEISCHER, *J. Appl. Phys.* **33**. (1962) 3504.
25. P. L. PRATT, R. CHANG and C. W. A. NEWEY, *Appl. Phys. Letters.* **3** (1963) 83.
26. W. FRANK, *Phys. Stat. Solidi.* **29** (1968) 391.
27. *Idem, ibid* **29** (1968) 767.
28. R. CHANG and L. J. GRAHAM, *Acta Cryst.* **17** (1964) 795.
29. J. S. NADEAU, *Can. J. Phys.* **45** (1967) 827.
30. J. FRIEDEL, "Dislocations" (Addison-Wesley, Reading, Mass. 1964) p. 225.
31. A. J. E. FOREMAN and M. J. MAKIN, *Phil. Mag.* **14** (1966) 911.
32. F. GUIU and T. G. LANGDON, *ibid* **30** (1974) 145.
33. R. J. ARSENAULT and R. DEWIT, *Acta Met.* **22** (1974) 819.
34. W. FRANK and A. SEEGER, "Symposium on the Interaction Between Dislocations and Point Defects", AERE-R 5944 Vol. 3, (Harwell, 1968) p. 682.
35. B. RAPPICH, *Acta Met.* **20** (1972) 557; *Mater. Sci. Eng.* **22** (1976) 71.
36. R. LABUSCH, *Acta Met.* **20** (1972) 917.
37. K. ONO, "Proceedings of 3rd International Conference on Strenght of Metals and Alloys", (Cambridge, England, 1973).
38. Edited by D. PECKNER, (Reinhold, New York, 1964) p. 93.
39. M. SRINIVASAN and T. G. STOEBE, *J. Appl. Phys.* **41** (1970) 3726.
40. J. SNOEK, *Physica* **8** (1941) 711.

Received 21 July and accepted 16 December 1976.